

RESEARCH COMMUNICATION

Loss of *Dis3l2* partially phenocopies Perlman syndrome in mice and results in up-regulation of *Igf2* in nephron progenitor cells

Ryan W. Hunter,^{1,2} Yangjian Liu,^{1,13}
Hema Manjunath,¹ Asha Acharya,¹
Benjamin T. Jones,¹ He Zhang,^{3,4} Beibei Chen,^{3,4}
Harini Ramalingam,¹ Robert E. Hammer,⁵
Yang Xie,^{3,4,6} James A. Richardson,^{1,7}
Dinesh Rakheja,^{6,7,8,9} Thomas J. Carroll,^{1,6,10,11}
and Joshua T. Mendell^{1,6,11,12}

¹Department of Molecular Biology, ²Medical Scientist Training Program, ³Department of Clinical Sciences, ⁴Quantitative Biomedical Research Center, ⁵Department of Biochemistry, ⁶Harold C. Simmons Comprehensive Cancer Center, ⁷Department of Pathology, ⁸Department of Pediatrics, University of Texas Southwestern Medical Center, Dallas, Texas 75390, USA; ⁹Division of Pathology and Laboratory Medicine, Children's Health, Dallas, Texas 75235, USA; ¹⁰Department of Internal Medicine, ¹¹Hamon Center for Regenerative Science and Medicine, ¹²Howard Hughes Medical Institute, University of Texas Southwestern Medical Center, Dallas, Texas 75390, USA

Loss of function of the DIS3L2 exoribonuclease is associated with Wilms tumor and the Perlman congenital overgrowth syndrome. LIN28, a Wilms tumor oncoprotein, triggers the DIS3L2-mediated degradation of the precursor of let-7, a microRNA that inhibits Wilms tumor development. These observations have led to speculation that DIS3L2-mediated tumor suppression is attributable to let-7 regulation. Here we examine new DIS3L2-deficient cell lines and mouse models, demonstrating that DIS3L2 loss has no effect on mature let-7 levels. Rather, analysis of *Dis3l2*-null nephron progenitor cells, a potential cell of origin of Wilms tumors, reveals up-regulation of *Igf2*, a growth-promoting gene strongly associated with Wilms tumorigenesis. These findings nominate a new potential mechanism underlying the pathology associated with DIS3L2 deficiency.

Supplemental material is available for this article.

Received April 17, 2018; revised version accepted May 23, 2018.

Several lines of evidence strongly implicate the let-7 family of microRNAs (miRNAs) as important suppressors of Wilms tumor, the most common pediatric malignancy of

the kidney (Ward et al. 2014). Hot spot mutations in the miRNA-processing enzymes DROSHA and DICER that impair production of a subset of miRNAs, including let-7, are common in Wilms tumor (Rakheja et al. 2014; Torrezan et al. 2014; Walz et al. 2015; Wegert et al. 2015). Additionally, the negative regulator of let-7 maturation *LIN28B* is frequently overexpressed in advanced-stage Wilms tumors (Viswanathan et al. 2009), and overexpression of LIN28 in developing mouse kidneys leads to Wilms tumor-like pathology, which is suppressed by enforced expression of let-7 (Urbach et al. 2014). LIN28 inhibits let-7 maturation by binding to precursor let-7 (pre-let-7) hairpins, recruiting a terminal uridylyl transferase to catalyze the addition of a series of uridines to the pre-let-7 3' end (Supplemental Fig. S1A; Hagan et al. 2009; Heo et al. 2009). Uridylation of pre-let-7 serves as a trigger for degradation by DIS3L2 (Chang et al. 2013), an exoribonuclease that, interestingly, is also recurrently mutated in Wilms tumors (Astuti et al. 2012; Torrezan et al. 2014; Wegert et al. 2015; Gadd et al. 2017).

DIS3L2 is a highly conserved 3'–5' exoribonuclease that preferentially degrades uridylated RNA substrates (Chang et al. 2013; Lubas et al. 2013; Malecki et al. 2013; Ustianenko et al. 2013). In addition to pre-let-7, it has also been reported to target histone mRNAs and many small noncoding RNAs (Labno et al. 2016; Pirouz et al. 2016; Reimao-Pinto et al. 2016; Ustianenko et al. 2016). While somatic mutations in *DIS3L2* occur in sporadic Wilms tumors, germline mutations in *DIS3L2* result in Perlman syndrome, an overgrowth syndrome characterized by neonatal death, genitourinary (GU) anomalies, hypotonia, neurodevelopmental delay, and frequent Wilms tumors (Astuti et al. 2012; Higashimoto et al. 2013; Soma et al. 2017). *DIS3L2* mutations in both Perlman-associated and sporadic cases of Wilms tumor suggest the importance of this gene as a tumor suppressor, yet the mechanisms through which it functions as such remain unclear.

The importance of let-7 in Wilms tumorigenesis and the established role of DIS3L2 in LIN28-dependent let-7 repression have led many to postulate that DIS3L2 acts as a tumor suppressor by influencing let-7 expression (Chang et al. 2013; Urbach et al. 2014; Hohenstein et al. 2015; Wegert et al. 2015). However, our current understanding of the role of DIS3L2 in the LIN28 pathway is not congruent with this hypothesis (Supplemental Fig. S1B). For example, *Dis3l2* knockdown in embryonic stem (ES) cells results in accumulation of uridylated pre-let-7, but this species is not a substrate for DICER processing, and mature let-7 levels are accordingly unaffected by DIS3L2 inhibition in this cell type (Heo et al. 2008; Chang et al. 2013). Furthermore, since DIS3L2 is believed to be the terminal nuclease in the LIN28 pathway, the expected consequence of loss of this protein would be a potential increase in let-7 expression, an effect that would be expected to suppress, rather than enhance, Wilms tumor development. Nevertheless, knockdown of *DIS3L2* in HeLa cells was reported to result in reduced mature let-7 levels,

[**Keywords:** DIS3L2; *Igf2*; LIN28; Perlman syndrome; Wilms tumor; let-7; microRNA]

¹³Present address: Department of Developmental Biology, Washington University School of Medicine, St. Louis, MO 63110, USA.

Corresponding author: joshua.mendell@utsouthwestern.edu

Article published online ahead of print. Article and publication date are online at <http://www.genesdev.org/cgi/doi/10.1101/gad.315804.118>.

© 2018 Hunter et al. This article is distributed exclusively by Cold Spring Harbor Laboratory Press for the first six months after the full-issue publication date (see <http://genesdev.cshlp.org/site/misc/terms.xhtml>). After six months, it is available under a Creative Commons License (Attribution-NonCommercial 4.0 International), as described at <http://creativecommons.org/licenses/by-nc/4.0/>.

leading to speculation that this protein may act in a cell type-specific manner to regulate let-7 expression (Ustianenko et al. 2013).

Given the potentially paradoxical role of DIS3L2 in the LIN28–let-7 pathway and its role as a tumor suppressor in Wilms tumor, we sought to more thoroughly investigate the influence of DIS3L2 on let-7 expression in additional cell types, particularly those most relevant to Wilms tumor development. We observed that genetic inactivation of *DIS3L2* does not affect mature let-7 family members in a broad panel of mammalian cell lines. To address whether this holds true in relevant cell types in vivo, we generated two distinct conditional *Dis3l2* mutant mouse lines harboring a null allele that removes the DIS3L2 catalytic site or an allele modeled after the most commonly reported mutation in Perlman syndrome patients (Astuti et al. 2012; Higashimoto et al. 2013). Resultant phenotypes in both mouse models not only resemble some key Perlman syndrome features but also are indistinguishable from each other, providing evidence that disease-causing *DIS3L2* mutations observed in Perlman syndrome patients are phenotypically equivalent to null alleles. Moreover, examination of *Dis3l2*-null primary nephron progenitor cells (NPCs), a cell type proposed to be a Wilms tumor cell of origin (Huang et al. 2016), demonstrates that loss of this protein has no effect on mature let-7 expression in this context but rather results in up-regulation of *Igf2*, a principal Wilms tumor oncogene (Hu et al. 2011).

Results and Discussion

Loss of *DIS3L2* does not affect mature let-7 levels in cell lines

The effect of DIS3L2 loss on mature let-7 expression has thus far been examined in three cell types—mouse ES (mES) cells, HeLa cells, and P19 teratocarcinoma cells—exclusively using knockdown approaches (Chang et al. 2013; Ustianenko et al. 2013; Nowak et al. 2017). We first set out to examine whether DIS3L2 influences mature let-7 levels in a wider range of cell lines by using a genome-editing approach to completely eliminate DIS3L2 activity. Cell lines with undetectable LIN28A or LIN28B were selected (HeLa and HCT116), as were lines with varying levels of either LIN28A or LIN28B (E14tg2a [a mES cell line] and Igrov1 with LIN28A expression or HEK293T and Huh7 with LIN28B expression) (Fig. 1A). For each cell line, we used either transcription activator-like effector nuclease (TALEN) pairs or clustered regularly interspaced short palindromic repeats (CRISPR)/Cas9 to generate frameshifting insertion–deletion (indel) mutations in an early coding exon (Fig. 1B). In all examined *DIS3L2* knockout cell lines, confirmed by both DNA sequence analysis (Supplemental Fig. S2) and resultant loss of protein (Fig. 1C), mature let-7 levels remained comparable with parental cells (Fig. 1D,E). Notably, this included HeLa cells, where *DIS3L2* knockdown was reported previously to result in reduced let-7 abundance (Ustianenko et al. 2013). Consistent with prior reports, we did detect an increase in uridylated pre-let-7 in DIS3L2-deficient mES cells (Supplemental Fig. S3). These data indicate that, irrespective of LIN28 expression, DIS3L2 is not a major regulator of mature let-7 abundance in commonly used mammalian cell lines.

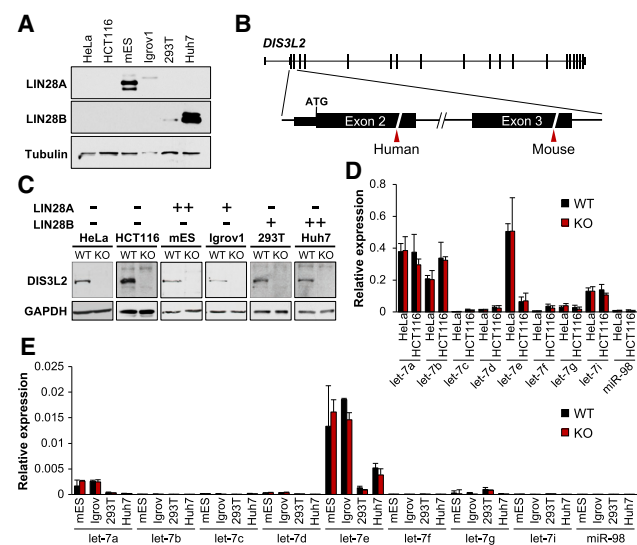


Figure 1. DIS3L2 loss does not affect mature let-7 levels in cell lines. (A) Western blot analysis of LIN28A/B. (B) Schematic of the gene-editing strategy used to generate *DIS3L2* knockout cell lines. Arrowheads indicate editing sites for human and mouse cells. (C) Western blot analysis of DIS3L2 in knockout and parental cell lines. (D,E) Quantitative RT-PCR (qRT-PCR) measurement of let-7 family members normalized to U6 in *DIS3L2* wild-type or knockout cell lines in which neither LIN28A nor LIN28B is expressed (D) or lines expressing either LIN28A or LIN28B (E). Due to the lower level of expression of let-7 family members in LIN28-expressing cell lines, these values were plotted separately. $n = 3$ biological replicates for each cell line assayed. Error bars for this and all subsequent figures represent standard deviations.

Dis3l2 loss of function partially recapitulates Perlman syndrome in mice

Although DIS3L2 deficiency did not influence mature let-7 levels in a broad panel of cell lines, it remained possible that loss of DIS3L2 results in altered let-7 expression in Wilms tumor-relevant cell populations within the context of the developing kidney. To investigate this possibility, we used CRISPR/Cas9 to generate mice with either conditional or germline-inheritable *Dis3l2* mutations. Given that Perlman syndrome-associated *DIS3L2* mutations are presumed to result in loss of function (Astuti et al. 2012), we initially generated a *Dis3l2*-null allele by targeting mouse exon 11 (orthologous to exon 10 of the human gene), which encodes highly conserved residues essential for catalytic activity (Fig. 2A; Chang et al. 2013) and whose deletion results in a frameshift and premature termination codon. Single-guide RNAs (sgRNAs) targeting sequences flanking exon 11 together with Cas9 mRNA and oligonucleotides containing loxP sites were coinjected into fertilized oocytes, resulting in the generation of both exon 11-deleted (*Dis3l2*^{Δ11}) and exon 11-flanked (*Dis3l2*^{11fl}) alleles.

Analysis of offspring derived from *Dis3l2*^{+/Δ11} intercrosses revealed fully penetrant perinatal lethality of *Dis3l2*^{Δ11/Δ11} mice, with no homozygous animals surviving the first postnatal day (Supplemental Table S1). Consequently, litters were delivered by caesarean section at embryonic day 18.5 (E18.5), revealing the presence of all genotypes at the expected Mendelian frequencies and grossly normal development of *Dis3l2*^{Δ11/Δ11} animals

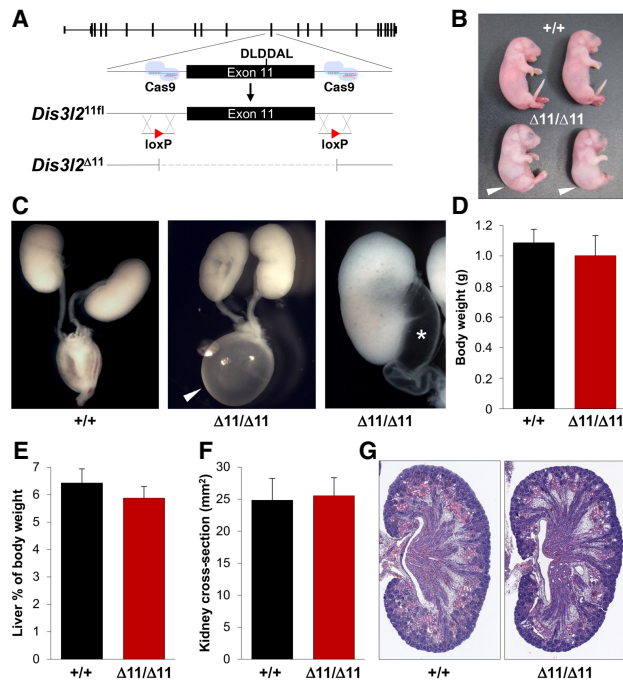


Figure 2. *Dis3l2* loss of function partially recapitulates Perlman syndrome in mice. (A) Strategy for generating exon 11-floxed (*Dis3l2*^{11fl}) and exon 11-deleted (*Dis3l2*^{Δ11}) alleles. Highly conserved residues in the DIS3L2 active site are indicated (DLDDAL). (B) Embryonic day 18.5 (E18.5) embryos of the indicated genotypes. Arrowheads mark abnormal curvature of the spine. (C) Representative images of a prematurely filled bladder (arrowhead) and hydronephrosis (asterisk) in E18.5 *Dis3l2*^{Δ11/Δ11} mice. (D,E,F) Total body weight (D), liver weight normalized to body weight (E), and kidney cross-sectional area (F) in E18.5 mice. *n* = 31–33 per genotype for whole body; *n* = 10–12 per genotype for livers; *n* = 6 per genotype for kidneys. (G) H&E-stained sections of E18.5 kidneys.

(Fig. 2B; Supplemental Table S1). Unlike caesarean-delivered *Dis3l2*^{+/+} and *Dis3l2*^{+/Δ11} mice, however, *Dis3l2*^{Δ11/Δ11} animals failed to initiate respiration, resulting in underinflated lungs (Supplemental Fig. S4) and rapid death. Consistent with the hypotonia commonly reported in Perlman syndrome, *Dis3l2*^{Δ11/Δ11} animals exhibited bradykinesia and abnormal curvature of the lumbar spine (Fig. 2B, arrowheads), a characteristic of neuromotor defects (Turgeon and Meloche 2009). Also consistent with Perlman syndrome, highly penetrant GU abnormalities, including hydronephrosis, hydronephrosis, and prematurely filled bladders, were present in knockout mice (Fig. 2C; Supplemental Table S2). Despite the presence of these Perlman syndrome features, overgrowth of E18.5 *Dis3l2*^{Δ11/Δ11} animals was not observed, and kidney development appeared overtly normal, without evidence of neoplastic pathology at this time point (Fig. 2D–G). Western blotting confirmed a loss of detectable DIS3L2 protein in *Dis3l2*^{Δ11/Δ11} kidneys (Supplemental Fig. S5).

Since *Dis3l2*^{Δ11/Δ11} animals die prior to the completion of nephrogenesis (Hartman et al. 2007), we used the conditional *Dis3l2*^{11fl} allele in combination with *Wt1*^{Cre}, which is expressed in the uninduced metanephric mesenchyme from which all nephrons and stroma of the kidney derive (Armstrong et al. 1993; Zhou et al. 2008), in

order to examine the consequences of DIS3L2 loss on later stages of kidney development. As expected, *Wt1*^{Cre/+}; *Dis3l2*^{11fl/11fl} mice exhibit efficient elimination of exon 11-containing *Dis3l2* mRNA in the kidneys (Supplemental Fig. S6A). Nevertheless, these animals survive into adulthood and display normal kidney histology without evidence of malignancy up to at least 6 mo of age (Supplemental Fig. S6B), a time point by which other Wilms tumor mouse models develop malignancies at high penetrance (Hu et al. 2011; Urbach et al. 2014). These findings demonstrate that loss of function of DIS3L2 in mice recapitulates some key features of Perlman syndrome, such as GU anomalies and neonatal death, but is not sufficient to impair kidney development or initiate Wilms tumor formation.

Modeling the most common Perlman syndrome mutation in mice

Although it is widely assumed that Perlman syndrome results from complete loss of function of DIS3L2, the failure of *Dis3l2*^{Δ11/Δ11} mice to recapitulate all aspects of this disorder led us to consider the possibility that disease-causing alleles may function as hypomorphs or neomorphs. Interestingly, among the reported Perlman syndrome mutations, the majority is in-frame deletions or point mutations. Moreover, all genetically characterized Perlman syndrome patients who developed Wilms tumor carry at least one mutation of this type (Fig. 3A). To directly assess the phenotypic consequences of a disease-associated mutation, we again used CRISPR/Cas9 to produce deleted and floxed alleles of mouse *Dis3l2* exon 10 (*Dis3l2*^{Δ10} and *Dis3l2*^{10fl}, respectively) (Fig. 3B), which mimic deletion of human *DIS3L2* exon 9, the most common mutation observed in Perlman syndrome patients. Importantly, this deletion, which is associated with Wilms tumor development, preserves the DIS3L2 reading frame and removes only 1% of the residues in the catalytic RNB domain. Nevertheless, DIS3L2 protein levels were dramatically reduced in the kidneys of E18.5 *Dis3l2*^{Δ10/Δ10} mice, suggesting that this mutation destabilizes the protein (Supplemental Fig. S5). Accordingly, the phenotype of *Dis3l2*^{Δ10/Δ10} mice was indistinguishable from *Dis3l2*^{Δ11/Δ11} mice, with fully penetrant perinatal lethality associated with lung hypoinflation, bradykinesia, and spinal curvature indicative of neuromotor defects, GU abnormalities, and an absence of overgrowth or kidney neoplasms (Fig. 3C–I; Supplemental Fig. S4; Supplemental Tables S1, S2). These data indicate that Perlman syndrome-associated mutations are functionally equivalent to null alleles.

DIS3L2 does not regulate mature *let-7* in Wilms tumor-relevant cell populations in vivo

We next took advantage of our DIS3L2-deficient mouse lines to directly investigate whether loss of DIS3L2 influences mature *let-7* levels in Wilms tumor-relevant cell populations in the context of the developing kidney. For these studies, we adopted recently reported methods to isolate primary NPCs, a population of cells in the developing kidney that have the capacity to both self-renew and produce nephrons (Fig. 4A; Boyle et al. 2008; Kobayashi et al. 2008; Brown et al. 2015). Wilms tumor-initiating cells have been shown to express NPC marker

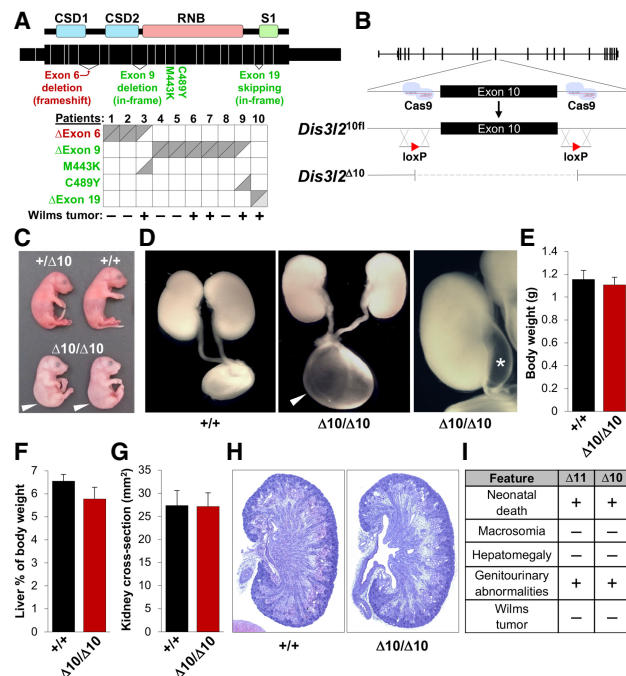


Figure 3. A Perlman syndrome-causing *Dis3l2* mutation phenocopies complete loss of function. (A) A schematic of DIS3L2 protein domains (top), the exon structure of the human *DIS3L2* gene showing the location of Perlman syndrome mutations (middle), and a table of alleles present in 10 Perlman syndrome patients showing the presence or absence of Wilms tumors (bottom). Note that patient 10 was heterozygous for the Δ Exon 19 allele but did not have detectable *DIS3L2* expression from the wild-type allele (Astuti et al. 2012). Red indicates a frameshift allele, and green represents a frame-preserving allele. (B) Strategy for generating exon 10 (orthologous to human exon 9) floxed (*Dis3l2*^{10fl}) and deleted (*Dis3l2*^{Δ10}) alleles. (C) E18.5 embryos of the indicated genotypes. Arrowheads mark abnormal curvature of the spine. (D) Representative images of a prematurely filled bladder (arrowhead) and hydronephrosis (asterisk) in E18.5 *Dis3l2*^{Δ10/Δ10} mice. (E, F, G) Total body weight (E), liver weight normalized to body weight (F), and kidney cross-sectional area (G) in E18.5 mice. $n = 10$ –11 per genotype for whole body; $n = 7$ –10 per genotype for livers; $n = 4$ per genotype for kidneys. (H) H&E-stained E18.5 kidney sections. (I) Summary of Perlman syndrome-associated phenotypes in *Dis3l2*^{Δ11/Δ11} and *Dis3l2*^{Δ10/Δ10} mice.

genes (Pode-Shakked et al. 2013), and Wilms tumors have been demonstrated to arise from NPCs in mouse models (Huang et al. 2016). Consistent with our earlier studies of *DIS3L2*-deficient cell lines, no significant differences in expression of mature let-7 family members were detected between NPCs derived from *Dis3l2*^{+/+} and *Dis3l2*^{Δ11/Δ11} mice (Fig. 4B).

To further investigate whether let-7 activity is affected by loss of *DIS3L2*, we performed RNA sequencing (RNA-seq) on littermate-matched *Dis3l2*^{+/+} and *Dis3l2*^{Δ11/Δ11} NPCs (Supplemental Table S3). These experiments demonstrated that expression of Targetscan-predicted let-7 target genes (Agarwal et al. 2015) was not globally altered in *Dis3l2*^{Δ11/Δ11} NPCs (Supplemental Fig. S7). Overall, these analyses of *DIS3L2* deficiency in a diverse panel of mammalian cell lines as well as in a primary cell population documented to give rise to Wilms tumors strongly implicate a let-7-independent mechanism of tumor suppression by *DIS3L2*.

DIS3L2 deficiency leads to *Igf2* overexpression in NPCs

To identify potential let-7-independent tumor suppressor functions of *DIS3L2*, we further examined the RNA-seq data from *Dis3l2*^{Δ11/Δ11} NPCs. As reported previously in other cell types (Labno et al. 2016; Pirouz et al. 2016; Reimao-Pinto et al. 2016; Ustianenko et al. 2016), we detected up-regulation of many histone mRNAs and RNA polymerase III (Pol III) transcribed small noncoding RNAs, including *Vaultrc5*, *Rny1*, *Rny3*, and *Rpph1* (Fig. 4C; Supplemental Table S3). Strikingly, among the most significantly up-regulated protein-coding genes was *Igf2*, along with the neighboring genes *H19* and *Igf2os*. This finding was noteworthy, as *IGF2* is recognized to be one of the most important Wilms tumor oncogenes. The *IGF2* locus is imprinted in nearly all tissues such that *IGF2* is transcribed exclusively from the paternal allele, while the neighboring *H19* gene is transcribed from the maternal allele. Loss of imprinting or loss of heterozygosity of this locus, resulting in *IGF2* overexpression, is observed in a majority of Wilms tumors (Wegert et al. 2015). Moreover, biallelic expression of *IGF2* underlies Beckwith-Wiedemann syndrome, an overgrowth syndrome with similarities to Perlman syndrome, including Wilms tumor susceptibility (Lapunzina 2005). Therefore, overexpression of *IGF2* could potentially contribute to both overgrowth and Wilms tumor development in Perlman syndrome. Quantitative RT-PCR (qRT-PCR) confirmed overexpression of both *Igf2* and *H19* in independently derived *Dis3l2*^{Δ11/Δ11} NPCs (Fig. 4D).

Given that *Igf2* and *H19* share a common set of enhancers (Nordin et al. 2014), their coordinated up-regulation in *DIS3L2*-deficient NPCs is most consistent with increased transcription of these genes. Indeed, we observed up-regulation of unspliced *Igf2* and *H19* transcripts in *Dis3l2*^{Δ11/Δ11} NPCs (Fig. 4E), strongly supporting this premise. Moreover, transcripts derived from all four annotated mouse *Igf2* promoters exhibited a proportional increase in expression, consistent with a general increase in transcription across the *Igf2/H19* locus (Supplemental Fig. S8). Since loss of imprinting is a common mechanism of increased *IGF2* transcription in Wilms tumor, we assessed the imprinting status of this locus in *Dis3l2* mutant NPCs. Intercrosses of C57BL/6 and BALB/cJ mice carrying the *Dis3l2*^{Δ11} allele allowed generation of NPCs with defined single-nucleotide polymorphisms (SNPs) in exons of *Igf2* and *H19* that were used to track allele-specific expression of each gene (Supplemental Fig. S9). Monoallelic expression of both *Igf2* and *H19* was observed in *Dis3l2*^{Δ11/Δ11} NPCs, demonstrating that loss of *DIS3L2* does not impact imprinting of this locus. We conclude that *DIS3L2* loss of function results in transcriptional activation of the *Igf2/H19* locus in NPCs, most likely by leading to the activation of shared *cis*-regulatory elements that control these genes.

IGF2: a new candidate driver of overgrowth and Wilms tumor in *DIS3L2*-deficient settings

The strong predisposition to Wilms tumor in Perlman syndrome as well as the presence of recurrent somatic mutations in *DIS3L2* in sporadic Wilms tumor provide compelling genetic evidence that this gene functions as a tumor suppressor in this malignancy. Given the role of *DIS3L2* as the terminal nuclease in the LIN28-let-7 pathway and the evidence linking the LIN28-let-7 pathway to

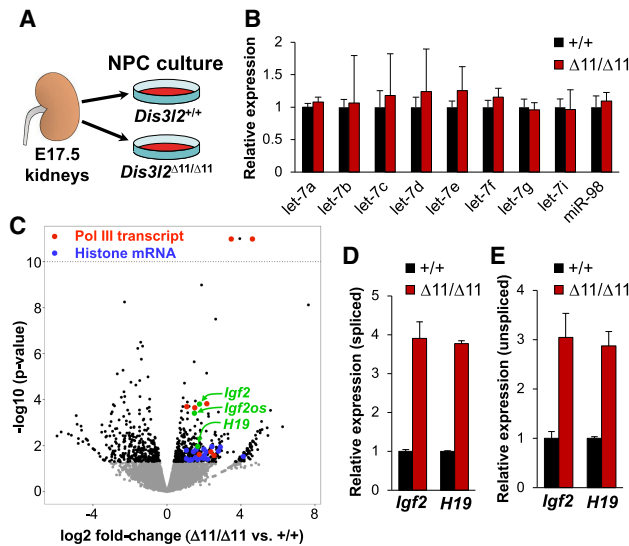


Figure 4. The effect of DIS3L2 loss of function on the NPC transcriptome. (A) Schematic of primary NPC culture derivation. (B) qRT-PCR measurements of let-7 family members normalized to U6 in *Dis3l2*^{+/+} and *Dis3l2*^{Δ11/Δ11} NPC cultures. *n* = 2 (let-7a and let-7f) or *n* = 3 (all others) independently derived NPC lines per genotype, each measured in triplicate. (C) Volcano plot depicting RNA sequencing results from *Dis3l2*^{+/+} and *Dis3l2*^{Δ11/Δ11} NPCs. EdgeR *P* < 10^{−10} for genes plotted above the dotted line. (D,E) qRT-PCR measurements of spliced (D) and unspliced (E) transcripts normalized to 18S in NPC cultures derived independently from those used in C. Error bars represent standard deviation of technical triplicates.

Wilms tumor pathogenesis, it has been widely speculated that altered let-7 expression underlies tumor formation in DIS3L2-deficient settings. In this study, we interrogated this hypothesis using the broadest set of cell types tested to date, including NPCs, a primary cell population of the developing kidney that has been demonstrated to give rise to Wilms tumors in mouse models. Our data unequivocally show that loss of DIS3L2 does not affect mature let-7 expression in these settings. Instead, using a novel *Dis3l2*-null mouse model, we uncovered *IGF2* as a novel candidate gene that could potentially drive fetal overgrowth and Wilms tumor in DIS3L2-deficient contexts. However, an important caveat of this model is that, while DIS3L2 loss of function in mice recapitulates some key Perlman syndrome-associated phenotypes, *Dis3l2*-null mice do not exhibit overgrowth or Wilms tumor development. The lack of overgrowth is most likely due to cell type specificity of *Igf2* regulation by DIS3L2, since we did not observe an increase in *Igf2* expression in the livers of *Dis3l2*^{Δ11/Δ11} mice (data not shown), and overexpression was not reported in previous RNA-seq studies of DIS3L2-deficient cell lines (Lubas et al. 2013; Labno et al. 2016; Ustianenko et al. 2016). It is plausible that *IGF2* is more broadly overexpressed in humans lacking DIS3L2, resulting in Perlman-associated overgrowth. Importantly, while genetic or epigenetic alterations of the *IGF2* locus have been ruled out as causes of Perlman syndrome (Alessandri et al. 2008; Astuti et al. 2012; Higashimoto et al. 2013), *IGF2* expression has not been directly examined in patients. Based on our findings reported here, it will be important to do so in the future, since targeting *IGF2* signaling could represent an effective therapeutic intervention.

The lack of tumor formation in *Dis3l2*-null mice is consistent with the previous demonstration that isolated *Igf2* overexpression is not sufficient to trigger Wilms tumor development in mouse models (Sun et al. 1997; Hu et al. 2011). Wilms tumors have been successfully generated in mice by combining multiple genetic lesions that co-occur in patients, such as *Igf2* loss of imprinting and *Wt1* deletion (Hu et al. 2011). Similar strategies using the new conditional *Dis3l2* mutant alleles reported here in combination with co-occurring Wilms tumor mutations in genes such as *DGCR8*, *WTX*, and others (Torrezan et al. 2014; Wegert et al. 2015; Gadd et al. 2017) are likely to produce new Wilms tumor models representing additional genetic subtypes of this malignancy. It is therefore anticipated that the new DIS3L2-deficient cell lines and mouse models generated in this study will provide a valuable resource for further study of the pathogenesis and treatment of Perlman syndrome and Wilms tumor.

Materials and methods

Mouse strains

Dis3l2 mutant alleles were generated using CRISPR/Cas9 as described previously (Yang et al. 2013). In brief, Cas9 mRNA (Sigma), in vitro transcribed sgRNA, and loxP-containing Ultramer oligos (Integrated DNA Technologies) were injected directly into C57BL/6J oocytes. Relevant oligonucleotide sequences are in Supplemental Table S4. Successfully generated alleles were maintained by backcrossing to C57BL/6J. *Wt1*^{Cre} (Zhou et al. 2008) and BALB/cJ mice were obtained from The Jackson Laboratory. All mouse experiments were approved by the Institutional Animal Care and Use Committee of the University of Texas Southwestern Medical Center.

Data access

RNA-seq data have been deposited in Gene Expression Omnibus under accession number GSE114673.

Acknowledgments

We thank Richard Gregory, Keith Joung, and Feng Zhang for plasmids and cell lines, and Vanessa Schmid in the McDermott Center Next-Generation Sequencing Core, John Shelton in the University of Texas Southwestern Histopathology Core, and Kathryn O'Donnell and Kenneth Chen for helpful discussions. This work was supported by grants from the Cancer Prevention and Research Institute of Texas (RP160249 to J.T.M., D.R., and T.J.C., and RP150596 to the University of Texas Southwestern Bioinformatics Core Facility), the National Institutes of Health (R35CA197311 to J.T.M.; R24DK080004, R01DK095057, R01DK106743, and P30DK079328 to T.J.C.; and P50CA196516 to Y.X., D.R., T.J.C., and J.T.M.), and the Welch Foundation (I-1961-20180324 to J.T.M.). H.R. was supported by a University of Texas Southwestern Center for Regenerative Science and Medicine fellowship. J.T.M. is an Investigator of the Howard Hughes Medical Institute.

Author contributions: R.W.H., Y.L., H.M., A.A., and B.T.J. performed experiments. H.Z., B.C., and Y.X. performed bioinformatic analyses. H.R. and T.J.C. assisted with NPC culture. R.W.H. and R.E.H. generated CRISPR/Cas9-edited mouse strains. R.W.H., A.A., J.A.R., D.R., T.J.C., and J.T.M. performed mouse phenotyping. R.W.H. and J.T.M. wrote the manuscript.

References

- Agarwal V, Bell GW, Nam JW, Bartel DP. 2015. Predicting effective micro-RNA target sites in mammalian mRNAs. *Elife* 4: e05005.
- Alessandri JL, Cuillier F, Ramful D, Ernould S, Robin S, de Napoli-Cocci S, Riviere JP, Rossignol S. 2008. Perlman syndrome: report, prenatal findings and review. *Am J Med Genet A* 146A: 2532–2537.

- Armstrong JF, Pritchard-Jones K, Bickmore WA, Hastie ND, Bard JB. 1993. The expression of the Wilms' tumour gene, WT1, in the developing mammalian embryo. *Mech Dev* **40**: 85–97.
- Astuti D, Morris MR, Cooper WN, Staals RH, Wake NC, Fewes GA, Gill H, Gentle D, Shuib S, Ricketts CJ, et al. 2012. Germline mutations in DIS3L2 cause the Perlman syndrome of overgrowth and Wilms tumor susceptibility. *Nat Genet* **44**: 277–284.
- Boyle S, Misfeldt A, Chandler KJ, Deal KK, Southard-Smith EM, Mortlock DP, Baldwin HS, de Caestecker M. 2008. Fate mapping using Cited1–CreERT2 mice demonstrates that the cap mesenchyme contains self-renewing progenitor cells and gives rise exclusively to nephronic epithelia. *Dev Biol* **313**: 234–245.
- Brown AC, Muthukrishnan SD, Oxburgh L. 2015. A synthetic niche for nephron progenitor cells. *Dev Cell* **34**: 229–241.
- Chang HM, Triboulet R, Thornton JE, Gregory RI. 2013. A role for the Perlman syndrome exonuclease Dis3l2 in the Lin28-let-7 pathway. *Nature* **497**: 244–248.
- Gadd S, Huff V, Walz AL, Ooms A, Armstrong AE, Gerhard DS, Smith MA, Auvil JMG, Meerzaman D, Chen QR, et al. 2017. A Children's Oncology Group and TARGET initiative exploring the genetic landscape of Wilms tumor. *Nat Genet* **49**: 1487–1494.
- Hagan JP, Piskounova E, Gregory RI. 2009. Lin28 recruits the TUTase Zcchc11 to inhibit let-7 maturation in mouse embryonic stem cells. *Nat Struct Mol Biol* **16**: 1021–1025.
- Hartman HA, Lai HL, Patterson LT. 2007. Cessation of renal morphogenesis in mice. *Dev Biol* **310**: 379–387.
- Heo I, Joo C, Cho J, Ha M, Han J, Kim VN. 2008. Lin28 mediates the terminal uridylation of let-7 precursor MicroRNA. *Mol Cell* **32**: 276–284.
- Heo I, Joo C, Kim YK, Ha M, Yoon MJ, Cho J, Yeom KH, Han J, Kim VN. 2009. TUT4 in concert with Lin28 suppresses microRNA biogenesis through pre-microRNA uridylation. *Cell* **138**: 696–708.
- Higashimoto K, Maeda T, Okada J, Ohtsuka Y, Sasaki K, Hirose A, Nomiya M, Takayanagi T, Fukuzawa R, Yatsuki H, et al. 2013. Homozygous deletion of DIS3L2 exon 9 due to non-allelic homologous recombination between LINE-1s in a Japanese patient with Perlman syndrome. *Eur J Hum Genet* **21**: 1316–1319.
- Hohenstein P, Pritchard-Jones K, Charlton J. 2015. The yin and yang of kidney development and Wilms' tumors. *Genes Dev* **29**: 467–482.
- Hu Q, Gao F, Tian W, Ruteshouser EC, Wang Y, Lazar A, Stewart J, Strong LC, Behringer RR, Huff V. 2011. Wt1 ablation and Igf2 upregulation in mice result in Wilms tumors with elevated ERK1/2 phosphorylation. *J Clin Invest* **121**: 174–183.
- Huang L, Mokkapat S, Hu Q, Ruteshouser EC, Hicks MJ, Huff V. 2016. Nephron progenitor but not stromal progenitor cells give rise to Wilms tumors in mouse models with β -catenin activation or Wt1 ablation and Igf2 upregulation. *Neoplasia* **18**: 71–81.
- Kobayashi A, Valerius MT, Mugford JW, Carroll TJ, Self M, Oliver G, McMahon AP. 2008. Six2 defines and regulates a multipotent self-renewing nephron progenitor population throughout mammalian kidney development. *Cell Stem Cell* **3**: 169–181.
- Labno A, Warkocki Z, Kulinski T, Krawczyk PS, Bijata K, Tomecki R, Dziembowski A. 2016. Perlman syndrome nuclease DIS3L2 controls cytoplasmic non-coding RNAs and provides surveillance pathway for maturing snRNAs. *Nucleic Acids Res* **44**: 10437–10453.
- Lapunzina P. 2005. Risk of tumorigenesis in overgrowth syndromes: a comprehensive review. *Am J Med Genet C Semin Med Genet* **137C**: 53–71.
- Lubas M, Damgaard CK, Tomecki R, Cysewski D, Jensen TH, Dziembowski A. 2013. Exonuclease hDIS3L2 specifies an exosome-independent 3'-5' degradation pathway of human cytoplasmic mRNA. *EMBO J* **32**: 1855–1868.
- Malecki M, Viegas SC, Carneiro T, Golik P, Dressaire C, Ferreira MG, Arraiano CM. 2013. The exoribonuclease Dis3L2 defines a novel eukaryotic RNA degradation pathway. *EMBO J* **32**: 1842–1854.
- Nordin M, Bergman D, Halje M, Engstrom W, Ward A. 2014. Epigenetic regulation of the Igf2/H19 gene cluster. *Cell Prolif* **47**: 189–199.
- Nowak JS, Hobor F, Downie Ruiz Velasco A, Choudhury NR, Heikel G, Kerr A, Ramos A, Michlewski G. 2017. Lin28a uses distinct mechanisms of binding to RNA and affects miRNA levels positively and negatively. *RNA* **23**: 317–332.
- Pirouz M, Du P, Munafo M, Gregory RI. 2016. Dis3l2-mediated decay is a quality control pathway for noncoding RNAs. *Cell Rep* **16**: 1861–1873.
- Pode-Shakked N, Shukrun R, Mark-Danieli M, Tsvetkov P, Bahar S, Pritchard S, Goldstein RS, Rom-Gross E, Mor Y, Fridman E, et al. 2013. The isolation and characterization of renal cancer initiating cells from human Wilms' tumour xenografts unveils new therapeutic targets. *EMBO Mol Med* **5**: 18–37.
- Rakheja D, Chen KS, Liu Y, Shukla AA, Schmid V, Chang TC, Khokhar S, Wickiser JE, Karandikar NJ, Malter JS, et al. 2014. Somatic mutations in DROSHA and DICER1 impair microRNA biogenesis through distinct mechanisms in Wilms tumours. *Nat Commun* **2**: 4802.
- Reimao-Pinto MM, Manzenreither RA, Burkard TR, Sledz P, Jinek M, Mechtler K, Ameres SL. 2016. Molecular basis for cytoplasmic RNA surveillance by uridylation-triggered decay in *Drosophila*. *EMBO J* **35**: 2417–2434.
- Soma N, Higashimoto K, Imamura M, Saitoh A, Soejima H, Nagasaki K. 2017. Long term survival of a patient with Perlman syndrome due to novel compound heterozygous missense mutations in RNB domain of DIS3L2. *Am J Med Genet A* **173**: 1077–1081.
- Sun FL, Dean WL, Kelsey G, Allen ND, Reik W. 1997. Transactivation of Igf2 in a mouse model of Beckwith-Wiedemann syndrome. *Nature* **389**: 809–815.
- Torrezan GT, Ferreira EN, Nakahata AM, Barros BD, Castro MT, Correa BR, Krepschi AC, Olivieri EH, Cunha IW, Tabori U, et al. 2014. Recurrent somatic mutation in DROSHA induces microRNA profile changes in Wilms tumour. *Nat Commun* **5**: 4039.
- Turgeon B, Meloche S. 2009. Interpreting neonatal lethal phenotypes in mouse mutants: insights into gene function and human diseases. *Physiol Rev* **89**: 1–26.
- Urbach A, Yermalovich A, Zhang J, Spina CS, Zhu H, Perez-Atayde AR, Shukrun R, Charlton J, Sebire N, Mifsud W, et al. 2014. Lin28 sustains early renal progenitors and induces Wilms tumor. *Genes Dev* **28**: 971–982.
- Ustianenko D, Hrossova D, Potesil D, Chalupnikova K, Hrazdilova K, Pachernik J, Cetkovska K, Uldrijan S, Zdrahal Z, Vanacova S. 2013. Mammalian DIS3L2 exoribonuclease targets the uridylated precursors of let-7 miRNAs. *RNA* **19**: 1632–1638.
- Ustianenko D, Pasulka J, Feketova Z, Bednarik L, Zigackova D, Fortova A, Zavolan M, Vanacova S. 2016. TUT-DIS3L2 is a mammalian surveillance pathway for aberrant structured non-coding RNAs. *EMBO J* **35**: 2179–2191.
- Viswanathan SR, Powers JT, Einhorn W, Hoshida Y, Ng TL, Toffanin S, O'Sullivan M, Lu J, Phillips LA, Lockhart VL, et al. 2009. Lin28 promotes transformation and is associated with advanced human malignancies. *Nat Genet* **41**: 843–848.
- Walz AL, Ooms A, Gadd S, Gerhard DS, Smith MA, Guidry Auvil JM, Meerzaman D, Chen QR, Hsu CH, Yan C, et al. 2015. Recurrent DGCR8, DROSHA, and SIX homeodomain mutations in favorable histology Wilms tumors. *Cancer Cell* **27**: 286–297.
- Ward E, DeSantis C, Robbins A, Kohler B, Jemal A. 2014. Childhood and adolescent cancer statistics, 2014. *CA Cancer J Clin* **64**: 83–103.
- Wegert J, Ishaque N, Vardapour R, Georg C, Gu Z, Bieg M, Ziegler B, Bausenwein S, Nourkani N, Ludwig N, et al. 2015. Mutations in the SIX1/2 pathway and the DROSHA/DGCR8 miRNA microprocessor complex underlie high-risk blastemal type Wilms tumors. *Cancer Cell* **27**: 298–311.
- Yang H, Wang H, Shivalila CS, Cheng AW, Shi L, Jaenisch R. 2013. One-step generation of mice carrying reporter and conditional alleles by CRISPR/Cas-mediated genome engineering. *Cell* **154**: 1370–1379.
- Zhou B, Ma Q, Rajagopal S, Wu SM, Domian I, Rivera-Feliciano J, Jiang D, von Gise A, Ikeda S, Chien KR, et al. 2008. Epicardial progenitors contribute to the cardiomyocyte lineage in the developing heart. *Nature* **454**: 109–113.



Loss of *Dis3l2* partially phenocopies Perlman syndrome in mice and results in up-regulation of *Igf2* in nephron progenitor cells

Ryan W. Hunter, Yangjian Liu, Hema Manjunath, et al.

Genes Dev. 2018, **32**: originally published online June 27, 2018
Access the most recent version at doi:[10.1101/gad.315804.118](https://doi.org/10.1101/gad.315804.118)

Supplemental Material <http://genesdev.cshlp.org/content/suppl/2018/06/27/gad.315804.118.DC1>

Related Content **Overgrowth syndromes and pediatric cancers: how many roads lead to IGF2?**
Ruthrothaselvi Bharathavikru and Nicholas D. Hastie
Genes Dev. August , 2018 32: 993-995

References This article cites 40 articles, 9 of which can be accessed free at:
<http://genesdev.cshlp.org/content/32/13-14/903.full.html#ref-list-1>

Articles cited in:
<http://genesdev.cshlp.org/content/32/13-14/903.full.html#related-urls>

Creative Commons License This article is distributed exclusively by Cold Spring Harbor Laboratory Press for the first six months after the full-issue publication date (see <http://genesdev.cshlp.org/site/misc/terms.xhtml>). After six months, it is available under a Creative Commons License (Attribution-NonCommercial 4.0 International), as described at <http://creativecommons.org/licenses/by-nc/4.0/>.

Email Alerting Service Receive free email alerts when new articles cite this article - sign up in the box at the top right corner of the article or [click here](#).

